Journal of Zhejiang University-SCIENCE C (Computers & Electronics)
ISSN 1869-1951 (Print); ISSN 1869-196X (Online)
www.zju.edu.cn/jzus; www.springerlink.com
E-mail: jzus@zju.edu.cn

Turning mechanism and composite control of stratospheric airships*

Mao-hua ZHANG[†1,2], Deng-ping DUAN[1,2], Li CHEN[†‡1,2]

([1]*Institute of Aerospace Science and Technology, Shanghai Jiao Tong University, Shanghai 200240, China*)

([2]*Institute of Aerospace Science and Technology Center of Ministry of Education, Shanghai 200240, China*)

[†]E-mail: superzhangmaohua@126.com; chenli2006@163.com

Received Mar. 26, 2012; Revision accepted July 31, 2012; Crosschecked Oct. 12, 2012

Abstract: The parametric model of stratospheric airships is established in the body axes coordinate system. In this paper we study the turning mechanism of stratospheric airships including the generated forces and the key parameters for steady turning. We compare and analyze the different driven-characteristics between aerodynamic control surfaces and vectored thrust in turning. We design a composite control combining aerodynamic control surfaces and vectored thrust according to different dynamic pressure conditions, to achieve coordinated turning under high or low airspeed situations.

Key words: Stratospheric airships, Horizontal turn, Composite control, Control allocation, Vectored thrust
doi:10.1631/jzus.C1200084 **Document code:** A **CLC number:** V249.121

1 Introduction

In the past few years, researchers have become increasingly interested in stratospheric airships because the main benefits of these aircraft are extended duration, high payload-to-weight ratio, low fuel cost, and recycling. Currently, United States, Japan, South Korea, and China are the major countries which develop stratospheric airships. The stratospheric airships are defined as lighter-than-air (LTA) vehicles with propulsion and steering systems in the stratosphere (between 20000 and 100000 m). Designing stratospheric airships is very challenging due to the extremely high altitude environment and significantly different from low altitude airship designs. Stratospheric airships have very large profiles and non-rigid structure and airship dynamics have inherent features such as fluid-solid coupling effect, buoyancy and added mass, and time-variation with altitude and airspeed (Masahiko and Masaaki, 2006; Lee and Bang, 2007; Miller and Sulliva, 2007; Mueller *et al.*, 2009). The resurgence of airships has created a need for accurate dynamics models and simulation capabilities to investigate the flight mechanism of stratospheric airships and to design their control systems (Kulczycki *et al.*, 2008).

In the flight mechanism of stratospheric airships, the turning mechanism is the most important. To increase the autonomous level of stratospheric airship operation, efficient, spot hover, and reliable trajectory planning capabilities are needed for researching the turning mechanism. However, most research focuses on the turning mechanism of airplanes and missiles. For those common aerial vehicles, there are two main ways for turning (Walden, 1994; Ben-Asher, 1995; Heymann and Ben-Asher, 1997; Yang and Kapila, 2002; Shiau *et al.*, 2010): skid-to-turn (STT) and bank-to-turn (BTT). In BTT, which is usually adopted by an unmanned aerial vehicle (UAV), the centripetal force for turning is generated from the lift, and the control maneuverability is poor for changing the attitude to obtain the component of lift. In STT, which is usually adopted by missiles, the centripetal force for turning is generated from the sliding force and the

‡ Corresponding author

* Project (No. 61175074) supported by the National Natural Science Foundation of China

control ability is low for generation of the sideslip angle. Because stratospheric airships are equipped with vectored thrust and aerodynamic control surfaces, and due to the lower flight speed, the turning mechanism of stratospheric airships is significantly different from that of the UAV and missiles (Khoury and Gillett, 2000). Therefore, we must have a thorough literature review on the study of airship dynamic models and the analysis of airship turning.

Many airship models have been described in the literature. Nippress and Gomes (1989) and Gomes (1990) generated the equations of motion of the YEZ-2A airship to construct the flight dynamics computer simulation model and enable estimation of the flight characteristics. Azinheira *et al.* (2002) investigated how to incorporate the wind effects into the nonlinear equations of motion of airships. Li *et al.* (2009) performed an analytical analysis of the aerodynamics of a flexible airship. Steady turning characteristics are a key aspect in the evaluation of the lateral maneuverability of airships. But in the literature, the part concerning steady turning characteristics of airships is scarce. Zhang *et al*. (2010) proposed an improved flight performance analysis method for analyzing the steady and accelerated performances of a hybrid airship. Li and Nabon (2007) and Li (2008) used a similar 2-DOF (degree-of-freedom) dynamics model to predict the steady turning rates for the Skyship-500, but these models of airships do not consider the effect of the vectored thrust. Hima and Bestaoui (2006) proposed an algorithm allowing the calculation of the trim trajectories for turning, in which actuator saturation is considered. Peddiraju *et al.* (2009) investigated the equations of motion for a fin-less airship; the vehicle can be stabilized using closed-loop thruster control. All these studies give the simulation results for turning control, but little effort has been put into the turning mechanism of the airship. Through establishment of a parametric model of stratospheric airships, in this paper we study the turning mechanism of stratospheric airships and the control allocation for turning from the viewpoint of manipulation.

2 Parametric dynamics of stratospheric airships

The aerodynamic configuration and arrangement of vectored thrust of one stratospheric airship studied here are shown in Fig. 1, including four aerodynamic control surfaces on the tail and two vectored thrusters on the left and right sides, respectively.

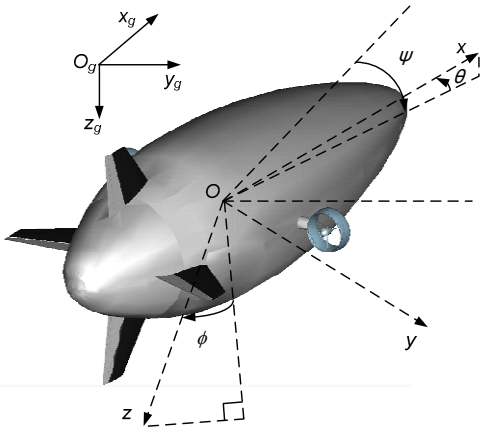

Fig. 1 The configuration of stratospheric airship

The thruster can be rotated by a vectored angle about the *y*-axis and produce two force components along the *x*- and *z*-axis in the longitudinal plane. When the rotational speeds of two thrusters are different, the differential yaw moment can be produced.

The turning of airships can be controlled by the differential thruster and the rudder. The control ability of the aerodynamic rudder is dependent on the airspeed, but the control ability of the differential thruster is independent of the airspeed, so the airship can realize the turning motion under different airspeeds even when airspeed is 0.

The vectored thrusters produce two force components and differential yaw moment, such that a control allocation among the two vectored thrusters and the rudder is needed.

The dynamics of aerostat is usually established in the body fixed frame for simplification. So, turning mechanism is also studied in the body fixed frame. For stratospheric airships, the gravity center of the airship is located much lower than the body center, such that the airship has a small pitch angle of less than 20°, and the roll angle is negligible. So, we still suppose the production of inertia I_{xy}=I_{yz}=0, as airship has a symmetric longitudinal plane, I_{xz} is small, and the coupling term of pitch with the yaw is $I_{xz}\times q\times r$ in the body frame (Khoury and Gillett, 2000), which can also be neglected as the gravity restored moment is very large.

In turning, ignoring the pitch and roll, and considering only the forward and lateral movements, the motion equation is simplified as (Nagabhushan and Pasha, 1992; Danowsky and Myers, 2008)

$$\begin{bmatrix} (m+m_{11})\dot{u} \\ -mz_G\dot{v}-I_{xz}\dot{r} \\ m_{26}\dot{v}+(I_z+m_{66})\dot{r} \end{bmatrix} = \begin{bmatrix} T_X+c_xq_\infty S_{\mathrm{ref}}+(m+m_{22})vr+(c_y^{\delta_r}\delta_{\mathrm{r}}+c_y^r r)q_\infty S_{\mathrm{ref}}\sin\beta \\ c_yq_\infty S_{\mathrm{ref}}+(c_y^{\delta_r}\delta_{\mathrm{r}}+c_y^r r)q_\infty S_{\mathrm{ref}}\cos\beta-(m+m_{11})ur \\ c_{\mathrm{n}}q_\infty S_{\mathrm{ref}}L_{\mathrm{ref}}+(c_{\mathrm{n}}^{\delta_r}\delta_{\mathrm{r}}+c_{\mathrm{n}}^r r)q_\infty S_{\mathrm{ref}}L_{\mathrm{ref}}+T_{\mathrm{D}} \end{bmatrix}, \tag{1}$$

where u, v, and r are the airship forward flight speed, lateral speed, and yaw rate, respectively, and m_{ij} is the additional mass for the airship. δ_{r} is the rudder deflection, T_X is the combined longitudinal thrust vector along the x-axis, and T_{D} is the differential moment vector around the z-axis. c_x, c_y, and c_{n} are the steady aerodynamic coefficients resulting from the airship hull, $c_y^{\,r}$ and $c_{\mathrm{n}}^{\,r}$ are the aerodynamic damping coefficients resulting from the yaw motion, and $c_y^{\delta_r}$ and $c_{\mathrm{n}}^{\delta_r}$ are the rudder effectiveness and the rudder control power, respectively. $S_{\mathrm{ref}}=V^{2/3}$ is the reference area and $L_{\mathrm{ref}}=V^{1/3}$ is the reference length, where V is the volume of the airship.

3 Turning mechanism of stratospheric airships

Different from the UAV, the weight of an airship is balanced with the buoyancy, the roll of airship is uncontrolled, and there is no wing to generate the lift. Thus, the turning is achieved by the rudder or by differentiating two side-vectored thrusts.

In the inertial frame, the equilibrium equation for steady turning is expressed as

$$F=mV^2/R=m\omega^2R,$$

where m is the mass, V is the turning speed, ω is the turning rate, R is the turning radius, and F is the centripetal force. When an airship is in steady skidding turning, the sideslip angle is constant, and then $\omega=r$ can be deduced (In Fig. 2, $\Omega+\Psi=180°$, and thus $\Psi=\Phi$). Thus, the centripetal force has the following equilibrium expression:

$$mV^2/R=m\omega^2R=mr^2R. \tag{2}$$

3.1 Steady turning driven by the rudder

The rudder is considered individually in steady turning and the motion Eq. (1) can be simplified as

$$\begin{cases} (m+m_{22})vr+T_X+c_xq_\infty S_{\mathrm{ref}}+(c_y^{\delta_r}\delta_{\mathrm{r}}+c_y^r r)q_\infty S_{\mathrm{ref}}\sin\beta=0, \\ c_yq_\infty S_{\mathrm{ref}}+(c_y^{\delta_r}\delta_{\mathrm{r}}+c_y^r r)q_\infty S_{\mathrm{ref}}\cos\beta-(m+m_{11})ur=0, \\ c_{\mathrm{n}}q_\infty S_{\mathrm{ref}}L_{\mathrm{ref}}+(c_{\mathrm{n}}^{\delta_r}\delta_{\mathrm{r}}+c_{\mathrm{n}}^r r)q_\infty S_{\mathrm{ref}}L_{\mathrm{ref}}=0. \end{cases} \tag{3}$$

The second lateral force equation can be rearranged as

$$\begin{aligned} &c_yq_\infty S_{\mathrm{ref}}+c_y^r rq_\infty S_{\mathrm{ref}}\cos\beta+c_y^{\delta_r}\delta_{\mathrm{r}}q_\infty S_{\mathrm{ref}}\cos\beta \\ &\quad=(m+m_{11})ur. \end{aligned} \tag{4}$$

The right-hand term $(m+m_{11})ur$ is the centrifugal force term that needs to be overcome. When the sideslip angle is zero, then $u=V$ and we have $(m+m_{11})ur=(m+m_{11})V^2/R$. When the sideslip angle is not zero, then $(m+m_{11})ur$ is part of the centrifugal force presented in the body frame (Fig. 2).

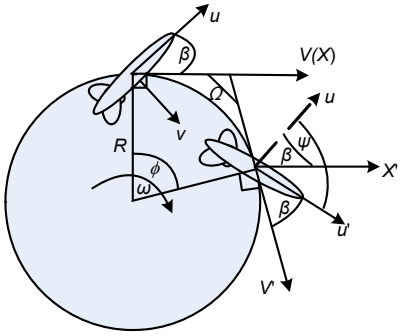

Fig. 2 Schematic diagram of the airship in steady turning

The left-hand terms are the centripetal force for turning, including the aerodynamic side force of hull $c_yq_\infty S_{\mathrm{ref}}$, the induced side force from the yaw and rudder deflection $c_y^{\,r}rq_\infty S_{\mathrm{ref}}\cos\beta$ and $c_y^{\,\delta_r}\delta_{\mathrm{r}}q_\infty S_{\mathrm{ref}}\cos\beta$. From Eq. (4), the steady forward speed u can be obtained for a given r, which can be decided uniquely by the last yaw equilibrium in Eq. (3). The yaw moment equilibrium equation is

$$c_{\mathrm{n}}q_\infty S_{\mathrm{ref}}L_{\mathrm{ref}}+c_{\mathrm{n}}^r rq_\infty S_{\mathrm{ref}}L_{\mathrm{ref}}=-c_{\mathrm{n}}^{\delta_r}\delta_{\mathrm{r}}q_\infty S_{\mathrm{ref}}L_{\mathrm{ref}}, \tag{5}$$

where $c_{\mathrm{n}}q_\infty S_{\mathrm{ref}}L_{\mathrm{ref}}$ is the aerodynamic yaw moment from the hull with its magnitude being decided by β,

and $c_n^r rq_\infty S_{ref} L_{ref}$ is the yaw damping moment. From the above expressions we can see that the turning angular velocity is $\omega=r$ and has no relation with the dynamic pressure q_∞, but is related to the aerodynamic coefficient c_n and c_n^r, and they are affected by the sideslip angle. When the turning rate ω is constant, turning radius $R=V/\omega$ is proportional to airspeed.

The longitudinal force equilibrium equation along the X-axis is given by

$$c_x q_\infty S_{ref} + (c_y^{\delta_r}\delta_r + c_y^r r) q_\infty S_{ref} \sin\beta = -T_X - (m+m_{22})vr, \tag{6}$$

where $c_x q_\infty S_{ref}$ is the resistance force needed to be overcome and $(c_y^{\delta_r}\delta_r + c_y^r r) q_\infty S_{ref} \sin\beta$ is the induced force along the X-axis due to the sideslip angle. T_X is the thrust along the X-axis, $(m+m_{22})vr$ is Carioles' force term caused by the sideslip and yaw motion, and the steady lateral speed can be obtained from this equation.

3.2 Steady turning driven by the vectored thrust

Consider the turning equation driven individually by the vectored thrust:

$$\begin{cases} c_x q_\infty S_{ref} + c_y^r r q_\infty S_{ref} \sin\beta = -T_X - (m+m_{22})vr, \\ c_y q_\infty S_{ref} + c_y^r r q_\infty S_{ref} \cos\beta = (m+m_{11})ur, \\ c_n q_\infty S_{ref} L_{ref} + c_n^r r q_\infty S_{ref} L_{ref} = -T_D. \end{cases} \tag{7}$$

Here the coupling between T_X and T_D must be considered:

$$T_l + T_r = T_X, \quad T_l - T_r = T_D / L_D, \tag{8}$$

where L_D is the moment arm of thruster, and T_l and T_r are the left and right vectored thrusts, respectively. When only the horizontal motion is considered, the vectored angle is at the initial zero position. Thus, the centripetal force for turning is provided by the lateral aerodynamic forces $c_y q_\infty S_{ref}$ and $c_y^r r q_\infty S_{ref}\cos\beta$, while the centrifugal force is generated from the coupling of the yaw rate r with the forward speed u.

3.3 Simulation results

The transitional processes of the airship from initial forward flight into turning driven by the rudder or the vectored thrust are depicted in Fig. 3.

Fig. 3 shows that as the heading is changed by the rudder, the flight speed is reduced and the turning radius of the transition process is reduced gradually, in order to achieve steady-state turning, as keeping speed is very important. The rudder is very suitable for turning control in case of high speed. If the speed cannot be maintained, there will be a great sideslip angle and a longer transition time. The higher the flight speed, the smaller the turning angular velocity, the smaller the sideslip angle, and the greater the turning radius.

Fig. 4 shows that the vectored thrust is very suitable for the turning in case of low speed. The

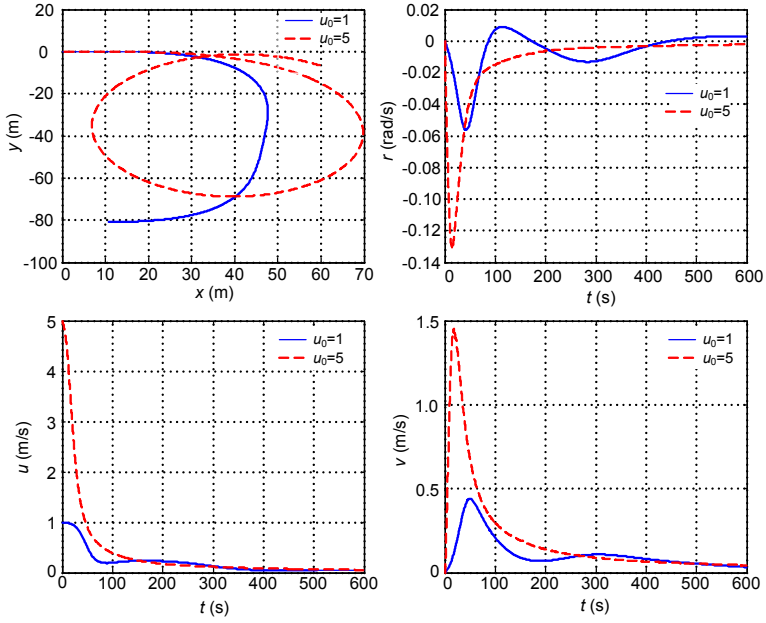

Fig. 3 The transitional turning course controlled by rudder (δ_r=10°)

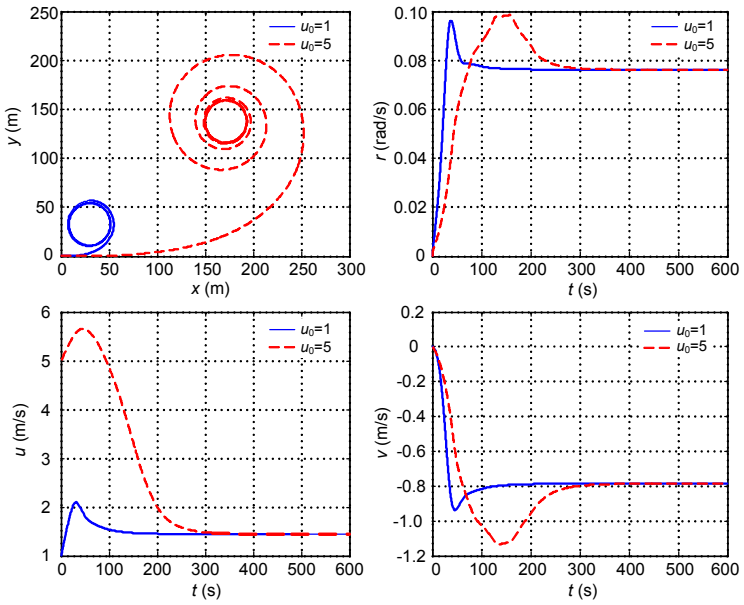

Fig. 4 The transitional course turning controlled by vectored thrust (TD=5000 nm)

greater the initial speed, the greater the turning radius, and the longer the transition time. The sideslip angle in turning driven by differential thrusters is lower than that when actuated by the rudder, and the turning rate is also lower.

4 Composite controls for heading control

The yaw moment generated from the rudder deflection δ_r is $c_n^{\delta_r}\delta_r q_\infty S_{ref} L_{ref}$, which is affected by the dynamic pressure. Figs. 3 and 4 show that when the steady forward speed is very slow, the output overshoot is small and the response is slow under the action of δ_r. However, under the action of vectored thrust, the response is fast, but overshoot is large. Therefore, in case of low speed, the rudder and the vectored thrust can be compensated in composite control for smooth turning; in case of high speed, the rudder has a high authority over the vectored thrust in consideration of energy consumption. Therefore, a control allocation strategy of yaw moment among the rudder and the vectored thrust can be deduced according to different dynamic pressures, and the weights of rudder (w_1) and vectored thrust (w_2) can be chosen as follows:

$$\begin{cases} w_1 = V / V_0, \quad w_2 = 1 - w_1, \quad V < V_0, \\ w_1 = 1, \quad w_2 = 0, \quad V \geq V_0, \end{cases} \tag{9}$$

where V_0 is a critical speed of the airship between the high and the low speeds. Critical speed is defined here as a speed dependent on the amplitude of the generated yaw moment. From the viewpoint of generated moment and consumed energy, a control allocation principle is proposed: when the airship is at an airspeed higher than the critical speed, the moment created by the rudder is large enough for yaw control. The power consumed by aerodynamic deflection is even smaller than by the thrust propeller; thus, the yaw is controlled by the rudder individually. When the airship is at an airspeed lower than the critical speed, the control allocation weight of yaw moment on the rudder is set as V/V_0. The control ability of the rudder is decreased with the airspeed, so the control weight disappears gradually with the airspeed, and the thruster is used for composite control to support the inadequate yaw moment. Here V_0=10 m/s can be determined from simulation. First, a control law can be designed for yaw channel from the commanded pitch angle to the expected yaw moment. Then the expected yaw moment is distributed among the differential vectored thrust and rudder according to the weights calculated from Eq. (9). Simulation results of composite control are shown in Fig. 5. Fig. 5a shows that the attitude response of an individual rudder is very poor. Because of the lower control ability, the rudder cannot go back from saturation. Fig. 5b shows that the attitude response of an individual vectored

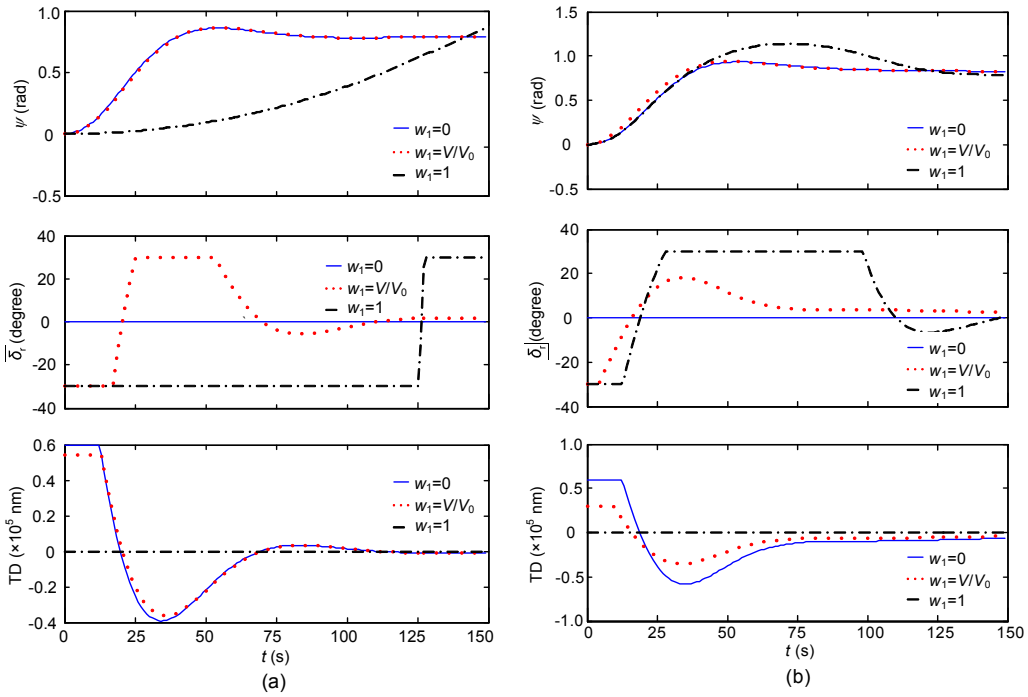

Fig. 5 Response of composite control at a flight speed of 1 m/s (a) or 5 m/s (b)

thrust has a little overshooting and that the required thrust is very high. Comparison of Figs. 5a and 5b shows that the response of composite control is smoother under different speeds and that the output of every actuator has smaller amplitude.

5 Conclusions

The turning mechanism of stratospheric airships is studied based on the parametric model established in the body frame. The component forces generated in steady turning are analyzed and the main factors impacting the turning characteristics are studied. The driving characteristics of the aerodynamic control surfaces and vectored thrust are compared and a control allocation method is proposed according to different dynamic pressures to achieve the coordinated turning in case of both high and low speeds. The main findings are as follows:

1. Rudder is very suitable for the turning in case of high speed. If the flight speed cannot be maintained, there will be a great sideslip angle and a long transition time. The higher the flight speed, the smaller the turning angular velocity, the smaller the sliding angle, and the greater the turning radius.

2. Vectored trust is very suitable for turning in the low-speed flight. The greater the speed, the greater the turning radius.

3. The composite control strategy can be designed for smooth turning, in which the expected yaw moment can be allocated to different actuators according to different dynamic pressures.

References

Azinheira, J.R., de Paiva, E.C., Bueno, S.S., 2002. Influence of wind speed on airship dynamics. *J. Guid. Control Dynam.*, **25**(6):1116-1124. [doi:10.2514/2.4991]

Ben-Asher, J.Z., 1995. Optimal trajectories for an unmanned air-vehicle in the horizontal plane. *J. Aircraft*, **32**(3):677-680. [doi:10.2514/3.46773]

Danowsky, B.P., Myers, T.T., 2008. Considerations in the Lateral Stability Characteristics of Airship Dynamics. AIAA Atmospheric Flight Mechanics Conf. and Exhibit.

Gomes, S.B.V., 1990. An Investigation of the Flight Dynamics of Airships with Application to the YEZ-2A. PhD Thesis, College of Aeronautics, Cranfield University, UK.

Heymann, V.I., Ben-Asher, J.Z., 1997. Aircraft trajectory optimization in the horizontal plane. *J. Guid. Control Dynam.*, **20**(6):1271-1274. [doi:10.2514/2.7602]

Hima, S., Bestaoui, Y., 2006. Trim Trajectories Characterization for an Unmanned Autonomous Airship. IEEE/RSJ Int. Conf. on Intelligent Robots and Systems, p.137-142. [doi:10.1109/IROS.2006.281930]

Khoury, G.A., Gillett, J.D., 2000. Airship Technology.

Cambridge University Press, Cambridge, UK.

Kulczycki, E.A., Johnson, J.R., Bayard, D.S., Elfe, A., Quadrell, M.B., 2008. On the Development of Parameterized Linear Analytical Longitudinal Airship Models. AIAA Guidance, Navigation and Control Conf. and Exhibit, p.769-774.

Lee, S., Bang, H., 2007. Three-dimensional ascent trajectory optimization for stratospheric airship platforms in the jet stream. *J. Guid. Control Dynam.*, **30**(5):1341-1351. [doi:10.2514/1.27344]

Li, Y., 2008. Dynamics Modeling and Simulation of Flexible Airships. PhD Thesis, McGill University, Montreal, Canada.

Li, Y., Nabon, M., 2007. Modeling and simulation of airship dynamics. *J. Guid. Control Dynam.*, **30**(6):1691-1700. [doi:10.2514/1.29061]

Li, Y., Nahon, M., Sharf, I., 2009. Dynamics modelling and simulation of flexible airships. *AIAA J.*, **47**(3):592-605. [doi:10.2514/1.37455]

Masahiko, O., Masaaki, S., 2006. Vehicle Proposal to Next Japanese Stratospheric LTA Developments. 6th AIAA Aviation Technology, Integration and Operations Conf.

Miller, C.J., Sulliva, J., 2007. High Altitude Airship Simulation Control and Low Altitude Flight Demonstration. AIAA Infotech@Aerospace Conf. and Exhibit.

Mueller, J.B., Zhao, Y., Garrard, W., 2009. Optimal ascent trajectories for stratospheric airships using wind energy. *J. Guid. Control Dynam.*, **32**(4):1232-1245. [doi:10.2514/1.41270]

Nagabhushan, B.L., Pasha, R.P.K., 1992. Analysis of airship lateral maneuverability. *J. Aircraft*, **29**(3):299-300. [doi:10.2514/3.46160]

Nippress, K.R., Gomes, S.B.V., 1989. Estimation of the Flight Dynamic Characteristics of the YEZ-2A. 8th Lighter-Than-Air Systems Technology Conf.

Peddiraju, P., Liesky, T., Nahon, M., 2009. Dynamics Modeling for an Unmanned, Unstable, Fin-Less Airship. 18th AIAA Lighter-Than-Air Systems Technology Conf.

Shiau, J.K., Ma, D.M., Shie, J.R., Chiu, C.W., 2010. Optimal sizing and cruise speed determination for a solar-powered airplane. *J. Aircraft*, **47**(2):622-629. [doi:10.2514/1.45908]

Walden, R., 1994. Time-optimal turn to a heading: an analytic solution. *J. Guid. Control Dynam.*, **17**(4):873-875. [doi:10.2514/3.21282]

Yang, G., Kapila, V., 2002. Optimal Path Planning for Unmanned Air Vehicles with Kinematic and Tactical Constraints. Proc. 41st IEEE Conf. on Decision and Control, p.1301-1306. [doi:10.1109/CDC.2002.1184695]

Zhang, K.S., Han, Z.H., Song, B.F., 2010. Flight performance analysis of hybrid airship: revised analytical formulation. *J. Aircraft*, **47**(4):1318-1330. [doi:10.2514/1.47294]